International Immunopharmacology 67 (2019) 176–185

Contents lists available at ScienceDirect

International Immunopharmacology

journal homepage: www.elsevier.com/locate/intimp

Novel antibody against oligomeric amyloid-β: Insight into factors for effectively reducing the aggregation and cytotoxicity of amyloid-β aggregates

Xiaoning Zhang[a,1], Yangyang Huai[a,1], Jing Cai[a,c], Chuli Song[a], Yingjiu Zhang[a,b,*]

[a] Key Laboratory for Molecular Enzymology and Engineering of the Ministry of Education, Jilin University, Changchun, China
[b] School of Life Science, Jilin University, Changchun, China
[c] China-Japan Union Hospital of Jilin University, Changchun, China

ARTICLE INFO

Keywords:
scFv antibody
Amyloid-β
Alzheimer's disease
Aggregation
Cytotoxicity

ABSTRACT

Amyloid-beta 42 (Aβ42) aggregates represent a prominent histopathological feature in Alzheimer's disease (AD); thus, immunotherapy against oligomeric Aβ42 aggregates is considered to be a potentially safe and specific therapeutic strategy. In this study, we identified an anti-oligomeric Aβ42 aggregate single-chain variable fragment (scFv) antibody, HT6, that is capable of efficiently binding to medium-sized Aβ42 aggregates (mainly 18–45 kDa) *in vitro* with an equilibrium dissociation constant (K_D) of 3.0×10^{-6} M, whether they were derived from Aβ42 monomer, larger Aβ42 oligomers, or even fibrils. This ability allowed scFv HT6 to induce the gradual disassembly of large Aβ42 aggregates into small Aβ42 oligomers while simultaneously effectively inhibiting the further development of Aβ42 aggregates. Moreover, the scFv HT6-targeted conformational region on Aβ42 aggregates was found to be more local and relatively close to the N-terminus of Aβ42; thus, scFv HT6 significantly delayed or even prevented the aggregation of Aβ42 protofibrils, while significantly reducing the cytotoxicity of Aβ42 oligomers. Overall, this study demonstrate that even though the decrease in the cytotoxicity of Aβ42 aggregates might be closely related to the reduction in Aβ42 aggregates and *vice versa*, the reduction in Aβ42 aggregates might not necessarily be accompanied by or followed by the reduction or even elimination of the cytotoxicity of Aβ42 aggregates. This insight enriches the diversity of anti-oligomeric Aβ42 antibodies, further providing a new understanding into the relationship between their binding pattern to Aβ42 aggregates and the efficacy against their formation, offering a therapeutic strategy to delay the progression of AD.

1. Introduction

Several signaling pathways are known to be impaired in patients with Alzheimer's disease (AD), and there is sufficient evidence that each mechanism can explain some aspects of the pathogenesis. However, the amyloidogenic mechanism, namely the toxic aggregation and deposition of amyloid-β (Aβ), and the amyloid-β oligomers (AβOs) mechanism are considered to be the most primary pathogenic causes of the disease [1,2].

Neurotoxic Aβ are peptides of 40–42 amino acids, and oligomeric Aβ1–42 (Aβ42) aggregates are considered to be relatively more toxic to nerve cells *in vivo* and *in vitro* than other forms. Therefore, formation of Aβ42 aggregates is considered to be the main causative initiator of AD [3]. Although other proteins such as tau protein have also been implicated in AD pathogenesis, there is evidence of a role of oligomeric Aβ42 in this mechanism as well, which can induce tau dysfunction [4–6]. Given that Aβ42 oligomers cause serious damage to human hippocampal neurons, they are an important therapeutic target for AD, especially at the early stage of the disease. Over the past three decades, immunotherapy against toxic Aβ42 targets has become an important part of AD treatment. Despite the lengthy, challenging, and laborious process of developing antibodies against neurotoxic Aβ42 targets, numerous studies have confirmed that anti-oligomeric Aβ42 antibodies, particularly anti-oligomeric Aβ42 single-chain variable fragment (scFv) antibodies, show therapeutic promise, with safety and specificity results indicating their potential suitability for clinical application in the

Abbreviations: Aβ42, amyloid-β (1–42); AD, Alzheimer's disease; CDR, complementarity determining region; scFv, single-chain variable fragment; VH, variable heavy; VL, variable light; ThT, thioflavin T; BSA, bovine serum albumin

* Corresponding author at: 2699 Qian-Jin Street, Changchun 130012, Jilin, China.
E-mail address: yingjiu@jlu.edu.cn (Y. Zhang).

[1] These authors are equal contribution.

https://doi.org/10.1016/j.intimp.2018.12.014
Received 6 September 2018; Received in revised form 6 November 2018; Accepted 5 December 2018
Available online 13 December 2018
1567-5769/

relatively near future.

Despite this progress, some key details concerning anti-oligomeric Aβ42 antibodies have not yet been revealed or remain to be elucidated, and it is clear that the detailed pathogenic role of oligomeric Aβ42 may be much more complicated than current models suggest. In order to break through the bottleneck of realizing an effective antibody-based treatment of AD, research efforts should focus on the diversity of anti-oligomeric Aβ42 antibodies to gain a more in-depth scientific understanding of the protective efficacy of antibodies. One of the main bottlenecks to resolve involves the variation in efficacies for inhibiting Aβ42 aggregation or cytotoxicity *in vitro* as well as cognitive protection *in vivo* among different conformation-recognized anti-oligomeric Aβ42 antibodies, *i.e.*, monoclonal antibodies or scFv antibodies that show similar specificity and affinity for toxic Aβ42 oligomers. In other words, even if anti-oligomeric Aβ42 antibodies have high specificity and affinity for Aβ42 aggregates, the properties may not be sufficient for inhibiting or eliminating their toxicity to brain neurons.

We previously reported the development of two anti-oligomeric Aβ42 scFv antibodies, designated scFv AS and scFv MO6, respectively, which can both specifically recognize oligomeric Aβ42 aggregates (AS: 25–55 kDa, MO6: 18–37 kDa) [7,8]. More importantly, both antibodies were shown to significantly attenuate the cytotoxicity of Aβ42 aggregates *in vitro* with similar binding characteristics to oligomeric Aβ42 aggregates in spite of their different primary structures. To further expand the diversity of Aβ42 antibodies, in the present study, we characterized another potent anti-oligomeric Aβ42 scFv antibody, HT6, which possesses the same heavy-chain variable domain (VH) as scFv MO6 but has a very different light-chain variable domain (VL) than scFv AS or scFv MO6. We characterized the unique efficacy and mode of action of scFv HT6 with the ultimate goal of providing new insight into the correlations between the structure or binding pattern and function of anti-toxic Aβ42 antibodies, which is expected to promote their clinical application.

2. Materials and methods

2.1. Aβ42 species and cells

Three Aβ42 aggregates (oligomers, protofibrils and fibrils) were prepared from Aβ42 monomer (Nanjing Peptide Biotechnology Industry Co., Ltd., Nanjing, China), and confirmed by electron microscopy as described previously [9,10]. The human neuroblastoma cell line SH-SY5Y (ATCC® CRL-2266™) was used and cultured as described previously [7].

2.2. ScFv HT6 antibody and anti-Aβ42 antibody

Aβ42 oligomer-specific scFv clones were screened by using the human scFv antibody library we previously reported [8]. Clone HT6 was selected by its higher reactivity toward Aβ42 oligomers and was prepared using previously described methods [8]. The purity of scFv HT6 exceeded 96% as determined by 12% SDS-PAGE. Mouse anti-human-β-amyloid monoclonal antibody (B4) (sc-28365) was purchased from Santa Cruz Biotech, Inc. (Shanghai, China).

2.3. Examination of scFv HT6 recognition specificity to four Aβ42 species by dot blot and Western blot analyses

The recognition specificity of scFv HT6 for four Aβ42 species (monomers, oligomers, protofibrils and fibrils) was analyzed by dot-blot and Western blot procedures as described previously [8]. Briefly, for dot-blot analysis, all Aβ42 species were directly spotted onto nitrocellulose membrane and were probed with scFv HT6, then with primary anti-His antibody (1:1000 dilution) (sc-8036, Santa Cruz Biotech, Inc., Shanghai, China) and secondary HRP-conjugated goat-anti-mouse IgG (1:5000 dilution) (bs-0296G, Beijing Biosynthesis Biotechnology Co., Ltd., Beijing, China). The recognition specificity of scFv HT6 for four Aβ42 species was evaluated based on the color intensities of four Aβ42 dots by visual comparison or was semi-quantitatively determined by gray scanning analysis of dot images. For Western blot analysis, four Aβ42 species were resolved by 12% native-PAGE and then transferred to polyvinylidene difluoride (PVDF) membrane, and finally probed as described above.

2.4. Determination of scFv HT6 binding capacity to Aβ42 oligomers

The antigen binding capacity of scFv HT6 was evaluated according to the minimum amount of Aβ42 oligomers bound by scFv HT6 using sandwich ELISA as described previously [8]. Briefly, scFv HT6 was added into the wells of a 96-microwell plate at final concentrations of 1.7, 3.4×10^{-2}, 8.5×10^{-3}, 2.1×10^{-3}, 1.7×10^{-3}, 1.1×10^{-3}, and 5.5×10^{-4} μM and incubated overnight at 4 °C, then incubated with Aβ42 oligomers at 5.0×10^{-3} μM for 1 h at 37 °C, and finally probed with B4 antibody as described previously [8]. An scFv HT6 sample was considered positive if its OD value at 450 nm was greater than the sum of 0.2 plus the OD value of the control at 450 nm, and also 2.1-fold greater than the OD value of the control at 450 nm. Experiments were performed in triplicate.

2.5. Measurement of scFv HT6 binding affinity to Aβ42 oligomers

The binding affinity of scFv HT6 for Aβ42 oligomers was evaluated using the equilibrium dissociation constant (K_D) between scFv HT6 and Aβ42 oligomers according to the method established by Bertrand Friguet [11,12]. The K_D value between scFv HT6 and Aβ42 oligomers was measured by indirect competitive ELISA as described previously [7]. Briefly, Aβ42 oligomers at 10^{-10} to 10^{-4} M in 10-fold serial dilutions were respectively mixed with scFv HT6 (1.0×10^{-7} M) and incubated for 1 h at 37 °C. Then, 100-μL mixture per well was transferred into another well that was pre-coated with 10 μg/mL Aβ42 oligomers for 12 h at 4 °C, and incubated for additional 1 h at 37 °C. After washing with PBST buffer (PBS containing 0.1% Tween-20), the amount of the bound scFv HT6 was probed with anti-His antibody as described previously [7] and the absorbance of each well was measured at 450 nm. Experiments were performed in triplicate. K_D value equals the initial concentration of free Aβ42 oligomers (M) at which half of the scFv HT6 was bound to the fixed Aβ42 oligomers.

2.6. Measurement of Aβ42 aggregates by thioflavin T fluorescence assay

Based on the positive correlation between the fluorescence intensity of the ThT reagent and the content of cross β-sheet structure, the main supersecondary structure in Aβ42 aggregates, the extent of the aggregation of the four Aβ42 species (monomers, oligomers, protofibrils and fibrils) was measured using the thioflavin T (ThT)-fluorescence assay (ThT-F) as described previously [7].

2.7. Assessment of the protective efficacy of scFv HT6 against Aβ42-induced cytotoxicity by cell viability and lactate dehydrogenase release assays

Human neuroblastoma SH-SY5Y cells were seeded in 96-well plates (Corning) at approximately 1000 cells per well and cultured for 24 h in a 5% CO_2 atmosphere at 37 °C to allow attachment to the bottom of the wells, then incubated with each of four Aβ42 species and scFv HT6 for an additional 24 h at 37 °C. The cytoprotective effects of scFv HT6 were assessed by 3-(4,5-dimethylthiazol-2-yl)-2,5-diphenyltetrazolium bromide (MTT) cell viability and lactate dehydrogenase (LDH) release assays as described previously [7]. The cytotoxicity-inhibiting and cytotoxicity-neutralizing efficacies of scFv HT6 were analyzed by using target cells treated simultaneously or sequentially with each of four Aβ42 species and scFv HT6 as described previously [9,10].

2.8. Molecular docking

The crystal structure of Aβ42 was downloaded from the Protein Data Bank (PDB) (PDB ID: 1Z0Q). 3D structures of scFv HT6 and the molecular docking of the Aβ42 to scFv HT6 were built [13,14]. The structural integrities of the docking models were visually examined using Discovery studio (DS) Visualizer 3.1 (http://accelrys.com/products/discovery-studio/visualization-download.php), and were used to generate images of the complex structure.

2.9. Statistical analysis

Data were obtained from at least three independent measurements for each experimental condition and expressed as the means ± SD. Their statistical significance was analyzed by one-way ANOVA for multiple groups. p value < 0.05 was considered statistically significant.

3. Results

3.1. Preparation of scFv HT6

Aβ42 oligomers were used to screen Aβ42 oligomer-specific clone(s) from the human scFv antibody library constructed in our previous study [8]. A particular effective clone, named HT6, was selected by an indirect enzyme-linked immunoassay (ELISA) technique as described previously [7]. The amino acid sequence deduced from the nucleotide sequence of the HT6 clone indicated the complete structure of a conventional scFv antibody, which was composed of a VH domain (amino acids 1–126) and a VL domain (amino acids 142–249) joined by a 15-amino acid linker (amino acids 127–141). The scFv HT6 sequence has been submitted to the GenBank database under accession number MG385839.

We compared the amino acid sequences of scFv HT6 and scFv MO6 and found that scFv HT6 showed approximately 94% amino acid sequence identity with scFv MO6 (GenBank accession number: AIX97363), sharing the same VH domain but distinct VL domains. As shown in Fig. 1a, the alignment of VL amino acid sequences, the additional alkaline C-terminal region in scFv HT6 allows it to carry more positive charges than scFv MO6. The two VL domains showed only 84% sequence identity.

Like scFv MO6, scFv HT6 is also a monovalent antibody, as confirmed by our previously described method (data not shown) [7], which indicates that the VH and VL domains coordinate for the recognition and binding of oligomeric Aβ42. Thus, we hypothesized that the interaction of scFv HT6 with Aβ42 oligomers would show different features, including binding patterns, compared to scFv MO6, considering its longer and more alkaline C-terminal fragment located adjacent to the third complementarity-determining region of VL (VL-CDR3). The purified scFv HT6 had a molecular weight of approximately 31 kDa (shown in Fig. S1).

3.2. Binding specificity of scFv HT6 to four Aβ42 species

The binding specificity of scFv HT6 to four types of Aβ42 species (monomers, oligomers, protofibrils, and fibrils) was examined by dot blot and Western blot analyses, respectively. The dot blotting patterns (as shown in Fig. S2) showed that scFv HT6 preferably bound to Aβ42 oligomers and protofibrils and only weakly bound to Aβ42 fibrils and Aβ42 monomers, whereas B4 antibody (positive control) could bind to all four Aβ42 species relatively equally. Quantification of these interactions according to the relative gray scale values (Fig. 1b) showed that scFv HT6 has the strongest binding to Aβ42 oligomers. Similar results were obtained by Western blotting, which further clarified that scFv HT6 specifically recognizes and binds to Aβ42 aggregated from small oligomers to immature protofibrils (mainly 18–45 kDa), whereas B4 antibody could bind to all Aβ42 species without size distinction (Fig. 1c). This indicated that scFv HT6, like scFv MO6, is a conformation-dependent anti-oligomeric Aβ42 scFv antibody. However, the two antibodies would recognize different epitopes given that they recognize Aβ42 aggregates of different molecular weights (HT6: 18–45 kDa, MO6: 18–37 kDa) and also have distinct VL domains.

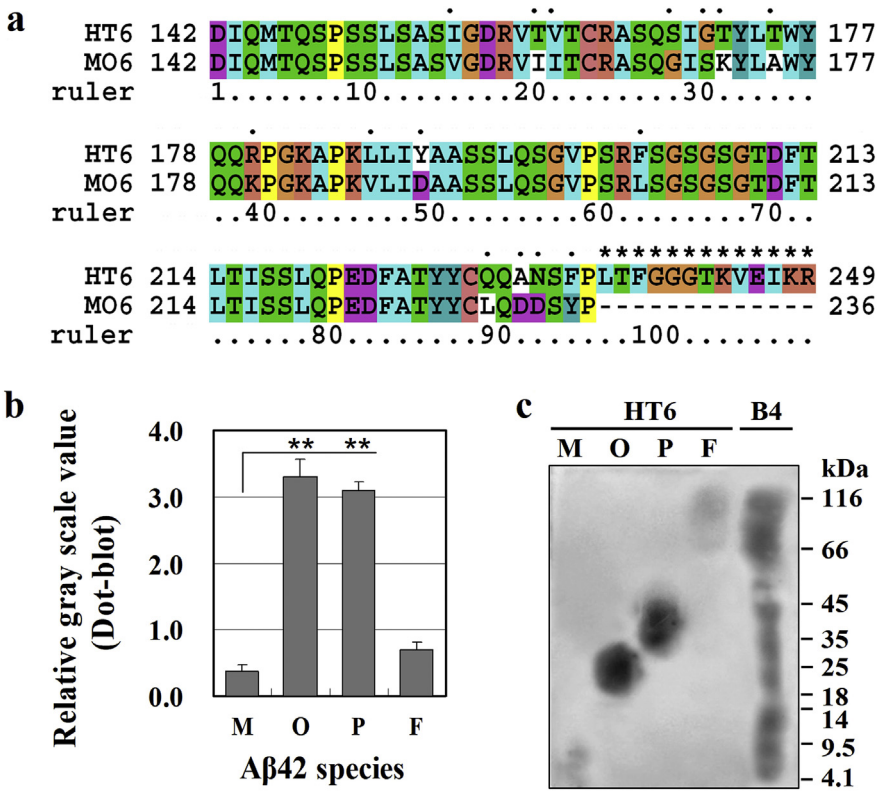

Fig. 1. Amino acid sequence alignment and specificity analysis of HT6. **a**: Comparation of the amino acid sequences of the VL domains of scFv HT6 (142–249 aa) and scFv MO6 (142–236 aa) (from reference [8]). Different amino acids were marked with black dots. The additional amino acids in the C-terminus of scFv HT6 were marked with asterisks. **b**: Semi-quantitative analysis of the dot blot images probed with scFv HT6. ** $p < 0.01$. **c**: Western blotting of the mixture of four Aβ42 species (monomers, M; oligomers, O; protofibrils, P; and fibrils, F) probed with B4 antibody (positive control).

The fact that scFv HT6 was able to recognize larger Aβ42 oligomers compared with scFv MO6 suggested that in high-molecular-weight Aβ42 oligomers, the conformational epitope recognized by scFv HT6 is more readily exposed or presented than that recognized by MO6.

3.3. Binding capacity of scFv MO6 to Aβ42 oligomers

Given the high specificity of scFv HT6 for Aβ42 oligomers, its binding capacity to Aβ42 oligomers could be assessed by determining the threshold concentration at which scFv HT6 bound effectively to Aβ42 oligomers. According to the definition of Section 2.4 in Materials and methods, the results (as shown in Fig. S3) verified that scFv HT6 could recognize and bind to Aβ42 oligomers at nanomolar concentrations, as low as 1.1 nM. However, scFv HT6 exhibited slightly weaker binding capacity to Aβ42 oligomers than scFv MO6, with a threshold concentration of Aβ42 oligomers of 0.625 nM [8].

3.4. Binding affinity of scFv HT6 for oligomeric Aβ42

In general, the binding affinity of an antibody for its antigen can be assessed by the equilibrium dissociation constant (K_D) between them. After establishing a series of equilibrium states between scFv HT6 and both the immobilized and free Aβ42 oligomers, the amounts of scFv HT6 bound to the immobilized Aβ42 oligomers on the plates were determined by indirect competitive ELISA, and the absorbance was measured at 450 nm to obtain the K_D values. The absorbance reached 50% of the maximum value at an Aβ42 oligomer concentration of approximately 3.0×10^{-6} M (as shown in Fig. S4), indicating that the K_D value for scFv HT6 was approximately 3.0×10^{-6} M. This value is smaller than the K_D value (5.2×10^{-6} M) of scFv MO6, indicating that scFv HT6 has higher binding affinity for Aβ42 oligomers.

3.5. ScFv HT6 reduces Aβ42 aggregation in vitro

To examine the ability of scFv HT6 to inhibit Aβ42 aggregation/Fibrillization, the extent of the aggregation of the four Aβ42 species (monomers, oligomers, protofibrils and fibrils) was monitored over 48 h using the thioflavin T-fluorescence (ThT-F) assay (shown in Fig. 2) and electron microscopy observation (shown in Fig. 3) in the presence or absence of scFv HT6. As shown in Fig. 2, in the presence of scFv HT6, the aggregation extents of all four Aβ42 species were distinctly reduced. Aβ42 monomers gradually aggregated into small Aβ42 oligomers (Fig. 2a), which would be recognized and captured by the co-incubated scFv HT6 to suppress the chance of any further aggregation of these nascent small Aβ42 oligomers. This finding confirmed that scFv HT6 effectively interacts with smaller Aβ42 oligomers rather than Aβ42 monomers, in line with the results of the specificity assay (Fig. 1b, c). In addition, the reduction profile of the aggregation of Aβ42 monomer using scFv HT6 was similar to that obtained using scFv MO6, indicating that these two antibodies have the same or similar efficacy for small Aβ42 oligomers.

Similarly, scFv HT6 not only suppressed the further aggregation of Aβ42 oligomers but also reversed their formation to some extent during the first 3 h of the reaction (Fig. 2b). This indicated that the specific binding of scFv HT6 to Aβ42 oligomers not only effectively inhibited the development of Aβ42 oligomers but also induced their disassembly into smaller Aβ42 oligomers. However, scFv HT6 showed the greatest efficacy in terms of both inhibiting development and inducing disassembly of aggregates in the Aβ42 protofibrils system within the first 3 h, despite a light increase in their aggregation after 3 h (Fig. 2c).

Finally, scFv HT6 had a similar but weaker effect on Aβ42 fibrils as observed on Aβ42 oligomers (Fig. 2d), suggesting that scFv HT6 could also slightly inhibit the growth of Aβ42 fibers or even induce a slight decrease in their aggregation, especially during the first 12 h.

The shapes and states of these Aβ42 above were further examined by electron microscopy after incubation of the four Aβ42 species with scFv HT6 for 24 h and the results were showed in Fig. 3. Aβ42 particles derived from co-incubation of Aβ42 monomers or oligomers with scFv HT6 (Fig. 3b or d) were much smaller than their corresponding controls (Fig. 3a or c), indicating that scFv HT6 effectively repressed Aβ42 aggregation while inducing the disassembly of the aggregates into smaller oligomers to a certain extent. Similar to the results of the ThT-F assay, even shorter or finer Aβ42 protofibrils, along with some Aβ42 oligomers, were observed when Aβ42 protofibrils were co-incubated with scFv HT6 (Fig. 3f) compared to the unique state of the corresponding controls (Fig. 3e). This further demonstrated the greater efficacy of scFv

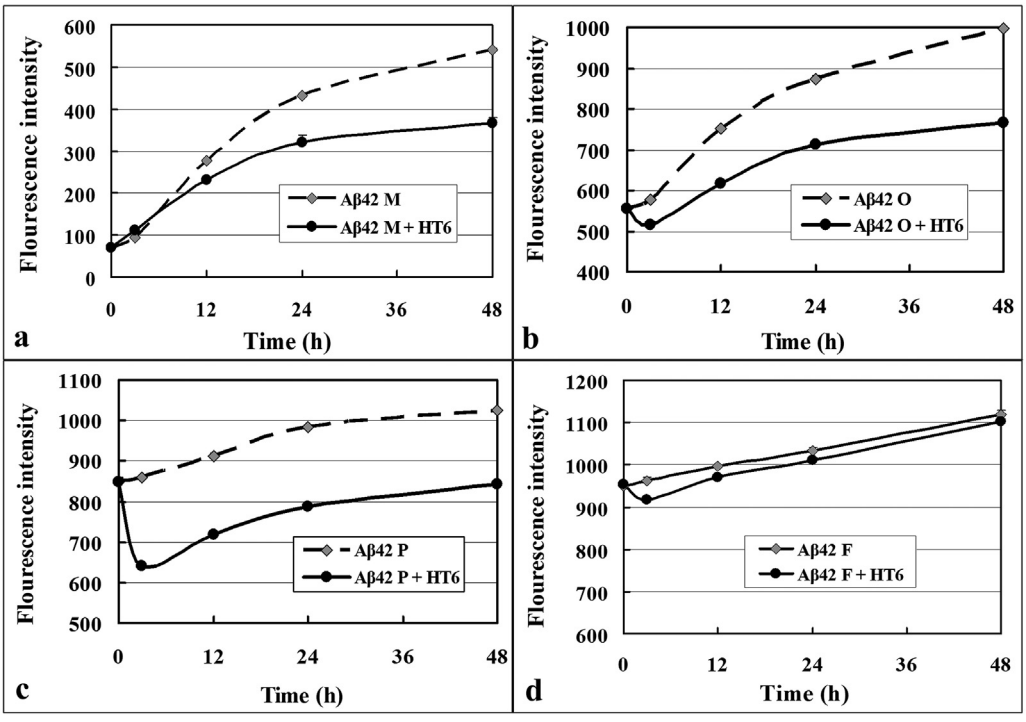

Fig. 2. ThT-F assay of four Aβ42 species (10 μM final concentration) after incubation with or without scFv HT6 (10 μM final concentration) at 37 °C for 3, 12, 24, or 48 h. Fluorescence intensity was measured at excitation and emission wavelengths of 450 nm and 482 nm, respectively. Each experiment was performed in triplicate. Values are presented as the means ± standard error of the mean (SEM). M, monomers; O, oligomers; P, protofibrils; F, fibrils.

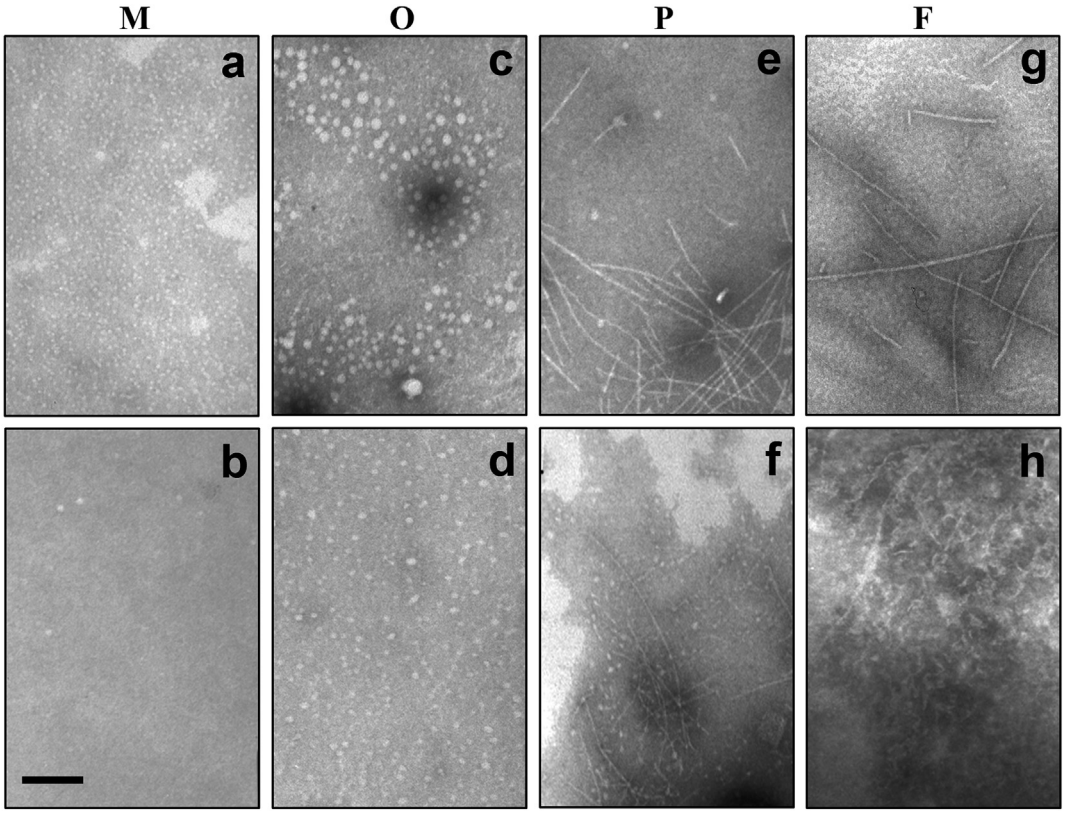

Fig. 3. Examination of shapes and states of four Aβ42 species (**a**, **b**: monomers, M; **c**, **d**: oligomers, O; **e**, **f**: protofibrils, P; **g**, **h**: fibrils, F) (10 μM final concentration each) by negative-stain electron microscopy after incubation with (bottom panels) or without (top panels) scFv HT6 (10 μM) at 37 °C for 24 h. All electron micrographs were recorded at a nominal magnification of 40,000× (scale bar, 100 nm).

HT6 in preventing the formation and stability of Aβ42 protofibrils. However, a mixture of diffuse and shorter or fine fibrillar states was observed when the Aβ42 fibrils were co-incubated with scFv HT6 (Fig. 3h) compared to their corresponding controls (Fig. 3g). These diffuse Aβ42 fibrils might represent the larger Aβ42–scFv HT6 complexes, from which the small Aβ42 oligomers might be subsequently dissociated out.

3.6. ScFv HT6 reduces the cytotoxicity of Aβ42 aggregates

Although an anti-Aβ42 antibody can exert its protective efficacy in many ways, Aβ42 antibodies are generally considered to protect their target cells *in vitro* and *in vivo via* their cytotoxicity-inhibiting and -neutralizing efficacies. To assess the physiological significance of scFv HT6, its Aβ42 cytotoxicity-inhibiting and -neutralizing efficacies against the four Aβ42 species were determined by MTT cell viability (shown in Fig. 4) and lactate dehydrogenase (LDH) release assays using SH-SY5Y cells.

The results in Fig. 4a demonstrated that scFv HT6 could reduce the cytotoxicity of all four Aβ42 species to varying degrees in a concentration-dependent manner. When the final concentration of scFv HT6 reached 10 μM, equal to that of Aβ42, 82% of the cells in the Aβ42 protofibrils system to 94% of the cells in the Aβ42 monomers system retained their viability compared to control cells (set to 100% cell survival). The LDH release of the target SH-SY5Y cells was monitored simultaneously with and without treatment of the four Aβ42 species and scFv HT6, which showed similar inhibition of Aβ42 cytotoxicity by scFv HT6 in each Aβ42 system (data not shown). This further confirmed that scFv HT6 could ameliorate or attenuate Aβ42-induced cell damage *in vitro* in a concentration-dependent manner.

The neutralization effect of scFv HT6 on Aβ42 cytotoxicity was also examined and compared to its inhibitory effect. As shown in Fig. 4a, scFv HT6 was more effective at inhibiting the Aβ42-induced cytotoxicity caused by the nascent Aβ42 oligomers resulting from Aβ42 monomers or Aβ42 fibrils (Fig. 3). In contrast, scFv HT6 showed almost identical inhibition and neutralization effects on the cytotoxicity of Aβ42 oligomers and Aβ42 protofibrils.

Furthermore, with increasing concentration of scFv HT6 (0.2–10 μM), the viability of cells in the Aβ42 oligomer or protofibril system increased much faster than that of cells in the Aβ42 monomer or Aβ42 fibril system, although the overall viability was consistently lower in the former two systems (Fig. 4a). This might be due to the higher binding affinity of scFv HT6 for Aβ42 oligomers and protofibrils (Fig. 1b, c) and the greater efficacy of scFv HT6 in inducing the disassembly of Aβ42 oligomers and protofibrils (Fig. 2). Therefore, there was no significant difference in the cell viability between the four Aβ42 systems when the concentration of scFv HT6 was increased to 10 μM (Fig. 4b), equimolar with Aβ42, although the protective effect of scFv HT6 in all four Aβ42 systems exhibited concentration dependence.

The protective efficacy of scFv HT6 was also reflected in maintaining the morphology of target cell *in vitro* (Fig. 4c). The cell images showed that scFv HT6 at a final concentration of 10 μM could effectively protected the morphology of target cells incubated with each of the four Aβ42 species (10 μM final concentrations, each), although the damage to target cell morphology induced by Aβ42 oligomers or protofibrils looked severe at a final concentration of 0.2 μM scFv HT6 (Fig. 4c). Furthermore, the results in Fig. 4c, particularly in the rows of Aβ42 oligomer and Aβ42 fibril of it, indicated that the protective effect of scFv HT6 on target cell morphology is also concentration dependent, which was consistent with the cases in Fig. 4a or in Fig. 2.

The results described above demonstrate the overall efficacy of scFv HT6, which is likely attributed to its robust and prolonged ability to capture Aβ42 owing to a good spatial fit (size and shape) and electrical matching. To obtain visual information about the interaction between

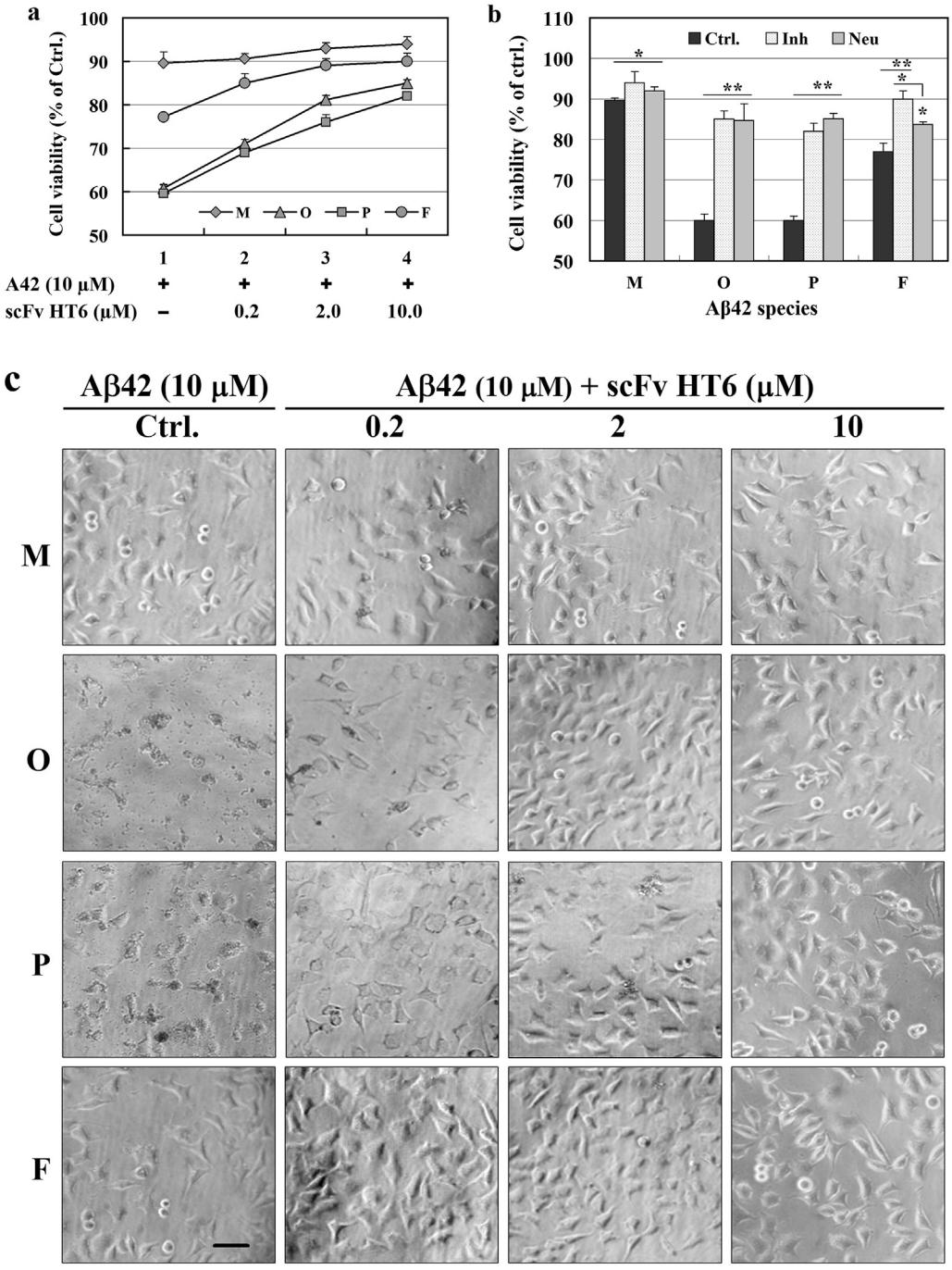

Fig. 4. Determination of the effect of scFv HT6 on Aβ42 cytotoxicity by MTT cell viability assay. **a**: Four Aβ42 species (10 μM final concentration each) with or without scFv HT6 (final concentration, 0.2-10 μM) were added to the wells pre-coated with SH-SY5Y cells. After 24 h of incubation, cell viability was measured by the MTT assay. **b**: Comparison of the neutralization and inhibition of Aβ42 cytotoxicity by scFv HT6. In the cytotoxicity-inhibiting groups, each Aβ42 sample and scFv HT6 were simultaneously added to each well (equal molarity), and the cells were cultured for 6 days. In the cytotoxicity-neutralizing groups, each Aβ42 sample was first added to each well and the cells were cultured for 3 days; the plates were then replenished with scFv HT6 (10 μM final concentration) and the cells were cultured for an additional 3 days. In the toxicity-control group, each Aβ42 sample was added to each well and the cells were cultured for 6 days. The blank control value was set to 100%. Each experiment was performed in triplicate. Values are presented as the means ± SEM. **c**: Morphologies and states of SH-SY5Y cells treated with four Aβ42 species (10 μM final concentration, each) or and scFv HT6 (0.2-10 μM final concentration) for six days. In toxicity control group, cells were cultured with each of the four Aβ42 species (10 μM final concentration) alone for 6 days. Bar, 100 μm. M: monomers, O: oligomers, P: protofibrils, F: fibrils, Inh: inhibiting, Neu: neutralizing, Ctrl, control.

scFv HT6 and Aβ42, molecular docking simulations were performed. The binding configuration of the scFv HT6–Aβ42 complex with the lowest energy was selected and further optimized by energy minimization. The final configuration of the docking complex of scFv HT6 and Aβ42 is shown in Fig. 5.

The docking model of the scFv HT6–Aβ42 complex clearly showed that the N-terminal half of the Aβ42 molecule (mainly amino acids 1–21) is embedded in the groove between the VL and VH domains of the scFv HT6 molecule (Fig. 5b to e) and lies close to the longer C-terminus of the VL domain (asterisks in Fig. 1a). However, the middle region of Aβ42 (mainly amino acids 22–30) immediately adjacent to the VH domain, and the C-terminal region of Aβ42 (mainly amino acids 31–42) are located outside of the complex entity. The C-terminal region (amino acids 29–42) of Aβ42 belongs to the transmembrane region, and thus its extension beyond the scFv HT6–Aβ42 complex (Fig. 5b, d, and e) indicated that the hydrophobic C-terminal regions in a small Aβ42 oligomer were close each other and formed their stable supersecondary structure. This configuration can explain the difference in that the pattern of interaction between Aβ42 and scFv HT6 from that observed between Aβ42 and scFv MO6 (Fig. 5f and g) [8].

This model further revealed that in addition to the van der Waals attraction between scFv HT6 and Aβ42, their interaction is mainly achieved by seven single and four double intermolecular hydrogen bonds (Fig. 5a), most of which (*i.e.*, three single bonds and four double bonds) were formed between the N-terminal region of Aβ42 (amino acids 1–14) and scFv HT6 (Fig. 5a). Furthermore, the participation of Gly241 and Lys244 of the longer C-terminus of scFv HT6 (Fig. 1) in the hydrogen bond network contributes to stabilizing the balance of interactions between Aβ42 and the VH domain and between Aβ42 and the VL domain. These interactions not only enable the N-terminal

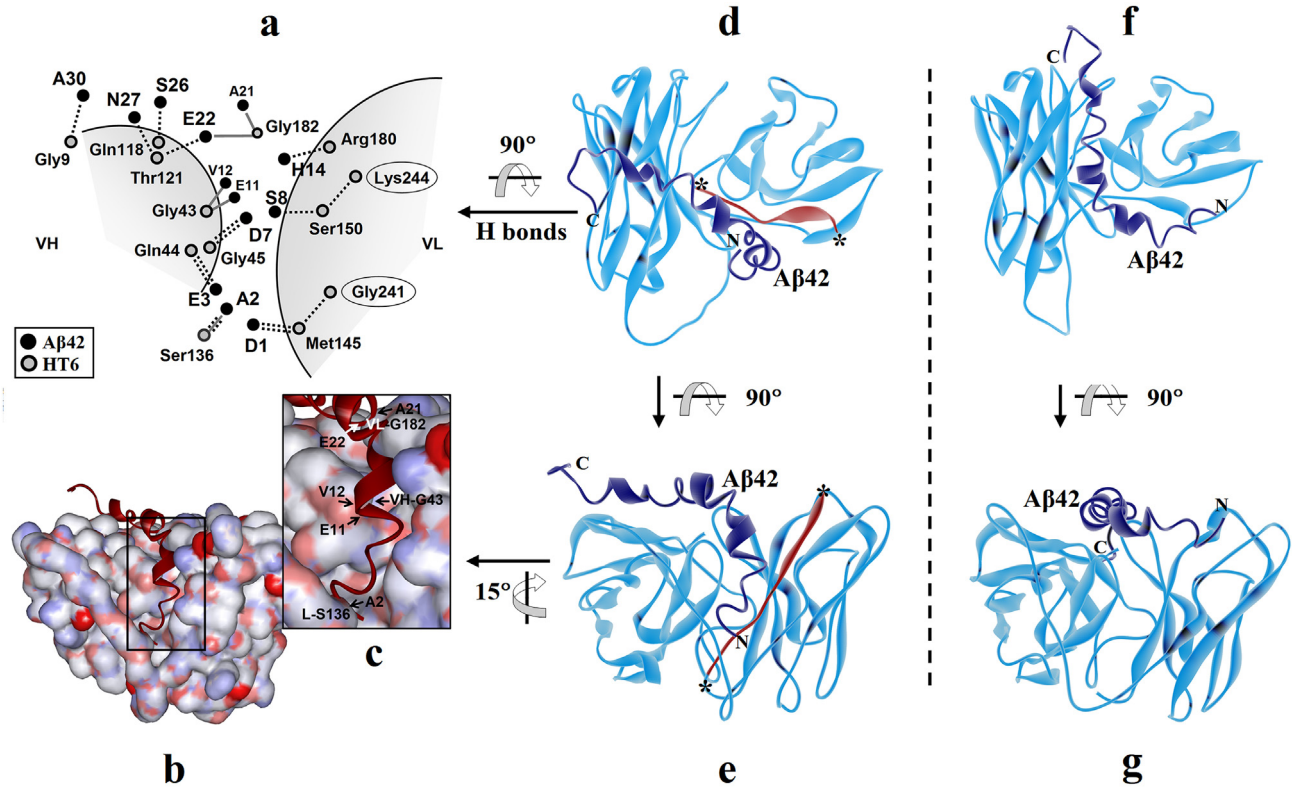

Fig. 5. Molecular docking model of an Aβ42 molecule to scFv HT6. **a**: Spatial arrangements and hydrogen-bond interactions (dashed lines) between amino acid residues of scFv HT6 (open circles and three-letter abbreviations) and Aβ42 (solid circles and single-letter abbreviations), and the tight interactions (light black solid lines) between residues A21-E22 and VL-Gly182, E11-V12 and VH-Gly43, and A2 and L-Ser136. Lys244 and Gly241 in the elliptical circles belonged to the C-terminal region of the VL domain. **b**: Surface representation of scFv HT6 in **a** or **e** with Aβ42 shown in ribbon mode. **c**: Enlarged image of the boxed area in **b**, showing the overlapping electron clouds between A21-E22 and VL-Gly182, E11-V12 and VH-Gly43, and A2 and L-Ser136. **d** and **e**: Ribbon display mode showing Aβ42 in dark color, scFv HT6 in light color, and the longer C-terminal region of the VL domain between two single asterisks (as marked with asterisks in Fig. 1a). **f** and **g**: Ribbon display mode of scFv MO6 with Aβ42 (from the reference [8]). N: N-terminus of Aβ42, C: C-terminus of Aβ42, H: hydrogen bond, L: linker.

region of the Aβ42 molecule to be anchored well in the groove between the VL and VH domains of the scFv HT6 molecule but also allow for the Ala21-Glu22 and Glu11-Val12 fragments and the Ala2 residue of Aβ42 to be very close to the VL-Gly182, VH-Gly43, and Linker-Ser136 regions, respectively, of scFv HT6 *via* the overlapping of electron clouds of their bonding electrons (Fig. 5c). This in turn results in very tight binding at the three sites (VL-Gly182, VH-Gly43, and Linker-Ser136) to consequently enhance the binding strength between scFv HT6 and Aβ42, surpassing that observed between scFv MO6 and Aβ42, as evidenced by their different K_D values (scFv HT6: 3.0×10^{-6} M; scFv MO6: 5.2×10^{-6} M).

4. Discussion

Through a series of *in vitro* experiments and simulations, we have confirmed scFv HT6 as a novel conformation-dependent anti-oligomeric Aβ42 scFv antibody. Although scFv HT6 has the same VH domain and a similar sequence to the VL domain of our previously reported Aβ42 scFv antibody MO6, they showed different properties and efficacies against oligomeric Aβ42 aggregates, which suggested that the VL domain might play a unique and important role in the recognition and binding to oligomeric Aβ42 aggregates. For example, scFv HT6 had a slightly weaker effect on the aggregation of Aβ42 oligomers but had a stronger effect on the aggregation of Aβ42 protofibrils or even fibrils (Fig. 1c, Fig. 2) compared with scFv MO6. This further suggests that in addition to low-molecular-weight Aβ42 oligomers, scFv HT6 could target slightly higher-molecular-weight Aβ42 oligomers or protofibrils compared to scFv MO6, demonstrating that scFv HT6 and MO6 recognize different conformational epitopes.

Based on the principle of protein–protein interactions, the recognition and binding between scFv HT6 or scFv MO6 and oligomeric Aβ42 aggregates, especially oligomers and protofibrils, should be based on their conformation complementarity in addition to their linear chemical interaction. Therefore, besides targeting different conformational epitopes on oligomeric Aβ42 aggregates, the scFv HT6-targeted region of Aβ42 might also be more local, uncovered on larger Aβ42 aggregates (up to 45 kDa), and thus more accessible. According to others and our previous reports [15–17], the N-terminal region (mainly amino acids 1–14) of Aβ42 is exposed to the outside of Aβ42 aggregates, while the hydrophobic C-terminal regions (mainly amino acids 30–42) of Aβ42 are closer to each other and form the hydrophobic core of the Aβ42 aggregates. Therefore, the scFv HT6-targeted region on oligomeric Aβ42 aggregates might be relatively closer to the N-terminus of Aβ42 than the scFv MO6-targeted region. This speculation was supported by the molecular docking simulation. In particular, comparison of Fig. 5d and f or Fig. 5e and g shows that the scFv MO6-targeted regions of Aβ42 are relative broader, which would not be conducive to the proximity and binding to larger Aβ42 aggregates.

Moreover, scFv HT6 had greater potency than scFv MO6 in restraining the development of Aβ42 aggregates, although both antibodies reduced the aggregation of Aβ42 monomer with the same efficacy [8]. In particular, scFv HT6 more effectively suppressed the development of Aβ42 protofibrils rather than Aβ42 oligomers, indicating that the hydrophobic interaction between the C-terminal regions of smaller Aβ42 oligomer subunits (such as the trimer (3-mer)) was stronger for larger Aβ42 oligomer particles (such as octadecamer (18-mer)) than in Aβ42 protofibrils. Consequently, separation of the smaller Aβ42 oligomer subunits induced by scFv HT6 was more readily

achieved from Aβ42 protofibrils than from larger Aβ42 oligomers because the scFv HT6-targeted region is relatively further from the C-terminus of Aβ42, even though scFv HT6 exhibited higher binding affinity for Aβ42 oligomers than scFv MO6. Furthermore, the results suggested that the C-terminal regions of the smaller Aβ42 oligomer subunits are buried inside the large Aβ42 oligomer particles, although this did not appear to be the case in Aβ42 protofibrils.

Like scFv MO6, scFv HT6 is a monovalent antibody, and thus its VH and VL domains together determine its recognition specificity and binding affinity. Accordingly, scFv HT6 and scFv MO6 would be expected to cause different changes in the properties or biological activities of Aβ42 aggregates due to their different VL domains. Indeed, scFv HT6 could effectively reduce the cytotoxicity of various Aβ42 species *in vitro*, particularly Aβ42 oligomers and Aβ42 protofibrils, by inhibiting and neutralizing Aβ42 cytotoxicity in a concentration-dependent manner. However, the efficacy of scFv HT6 against the cytotoxicity of Aβ42 oligomers was higher, albeit not much higher, than its efficacy against the cytotoxicity of Aβ42 protofibrils, which was inconsistent with its corresponding efficacy against Aβ42 aggregation. This implies that the scFv HT6-targeted site on Aβ42 aggregates has different associations with Aβ42 aggregation and cytotoxicity, respectively. Thus, it could be proposed that the critical conformational elements on Aβ42 aggregates responsible for Aβ42 aggregation and for Aβ42 cytotoxicity, respectively, might be different or at most only partially overlapping. This phenomenon is similar to the mechanism of enzyme inhibition. Competitive inhibitors of an enzyme directly inhibit the activity of the enzyme, whereas the non-competitive inhibitors indirectly inhibit the activity by inducing a conformational change in the non-active site or the regulatory site of the enzyme.

Many studies have suggested that specific sites on Aβ oligomers are involved in their cytotoxicity [18–21]. We previously reported that serum antibodies induced by Aβ1–28 or even Aβ1–9 fragments exerted a significant protection and restoration effect on target cells *in vitro* by inhibiting and neutralizing Aβ42-induced cytotoxicity. Based on all of the above analyses, judgments, and related reports [9,10,16,18,19,22,23], the N-terminal fragments of Aβ42 aggregates could be regarded as a neurotoxicity-inducing region, which could cause neuronal damage through one or more transmembrane signal transduction pathways [1,24]. To illustrate the relationship between the architectures of Aβ42 oligomers and protofibrils, antibody-targeting sites on Aβ42 aggregates, and the antibody's efficacies, we propose a rational model, which is depicted as a schematic diagram in Fig. 6, to show the distinct functional mechanisms of anti-oligomeric Aβ42 antibodies.

Aβ42 monomers (Aβ42-M in Fig. 6) tend to first form small Aβ42 oligomers such as Aβ42 trimers, which further aggregate to form larger Aβ42 aggregates under certain conditions. The architecture of a large Aβ42 oligomer (Aβ42-O in Fig. 6), similar to formation of a micelle by phospholipids, showed that the C-terminal fragments of small Aβ42 oligomers located inside interacted more strongly than those in Aβ42 protofibrils (Aβ42-P in Fig. 6), another subset of small Aβ42 oligomers. In addition to the hydrophobic interaction between the C-terminal fragments of small Aβ42 oligomers, the cross-linking between their N-terminal fragments might play an important role in stabilizing the architecture of protofibrils, similar to the base stacking forces in DNA.

In the Aβ42-O-antibody complex, the regions targeted by the antibody likely differs at the positions shown in Fig. 6a, b, or c, or further in the ranges indicated by the numbers 1, 2, and 3 in Fig. 6a, b, or c. Thus, the closer the antibody-targeted region is to the functional site or toxic site (responsible for Aβ42 cytotoxicity) on the N-terminal fragment of Aβ42 might lead to more effective action in reducing the cytotoxicity of Aβ42 aggregates, and *vice versa*. By contrast, with a broader antibody-targeted region, there is a lower probability that the region would be exposed outside of the high-molecular-weight Aβ42 aggregate, and thus it would be less likely to be recognized and bound by the antibody. However, a different or opposite situation might apply when considering the ability of the antibody to effectively reduce the aggregation of Aβ42. The other two related scFv antibodies, MO6 [8] and AS [7], also demonstrate the inferences above. The Fig. 7 briefly summarized the overall differences and similarities between the three scFvs HT6, MO6 and AS. Clearly, the effectiveness of an anti-oligomeric Aβ42 scFv antibody should depend on its overall efficacy against Aβ42 cytotoxicity.

Taken together, our results suggest that (1) in the interaction of a conformation-recognized anti-oligomeric Aβ42 scFv antibody with oligomeric Aβ42 aggregates, the conformational epitope recognized by the antibody might be inconsistent with the functional site (*i.e.*, the site responsible for cytotoxicity) on the Aβ42 aggregates, similar to enzyme inhibition, (2) even though the decrease in the cytotoxicity of Aβ42 aggregates might be closely related to the reduction in Aβ42 aggregates

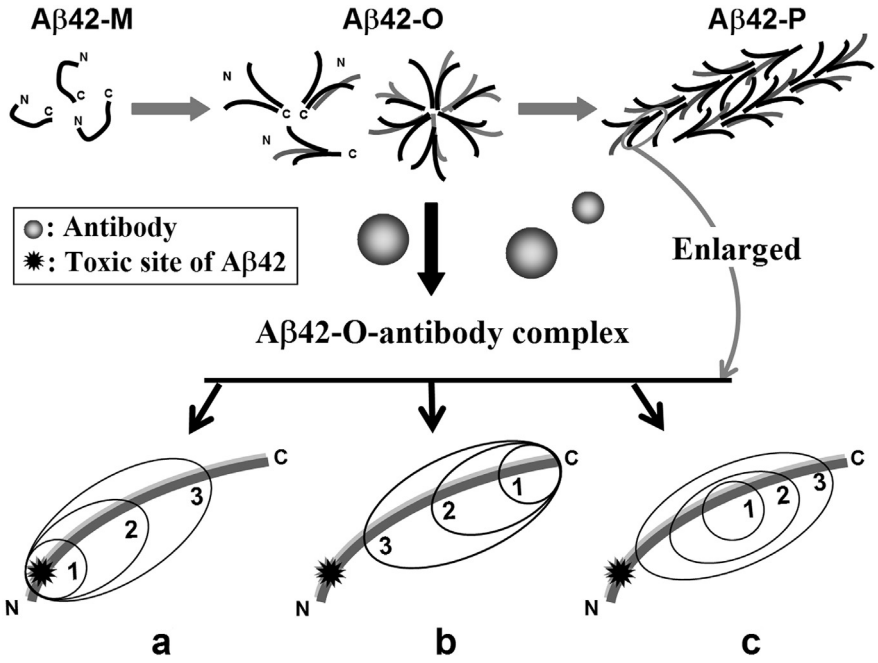

Fig. 6. Schematic diagram of Ab42 oligomers, Ab42 protofibrils and the possible conformational epitope regions targeted by anti-oligomeric Ab42 antibodies on Ab42 aggregates. Number 1 to 3: different antibody-targeted region represented by the corresponding circles; Gray sphere: anti-oligomeric Ab42 antibody; ✷: functional site or toxic site (responsible for Aβ42 cytotoxicity) in the N-terminal region of Ab42; M: monomers, O: oligomers, P: protofibrils; N-terminus of Aβ42, C: C-terminus of Aβ42.

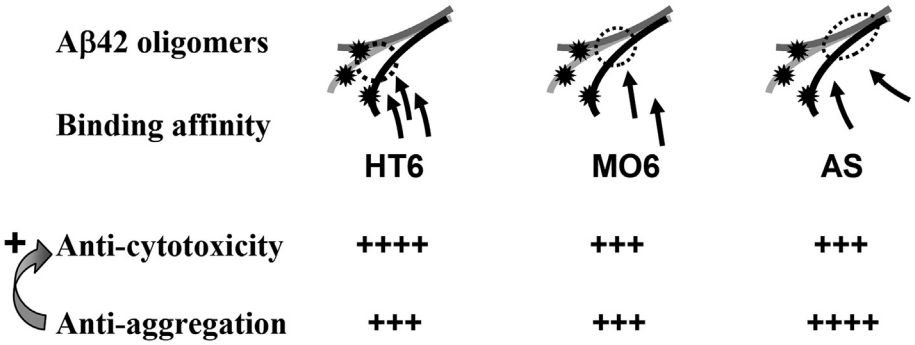

Fig. 7. Comparison of the overall efficacies of scFvs HT6, MO6 and AS on Ab42 oligomers (3-mer). The dotted ellipses on Ab42 oligomers (3-mer) indicated the region targeted by scFvs HT6, MO6 [8] or AS [7]. The black solid arrows indicated their binding affinity, and the grey U-turn arrow indicated promotion. ✷ was synonymous with that in Fig. 6.

and *vice versa*, these are physiologically or toxicologically distinct processes. In other words, the reduction in Aβ42 aggregates might not necessarily be accompanied by or followed by the reduction or even elimination of the cytotoxicity of Aβ42 aggregates.

Different antibodies might lead to different fates of these small Aβ42 oligomers. Maybe some antibodies would be like the newly reported anti-cancer antibodies [25], but the target here were not cancer cells but small Aβ42 oligomers. The subjective and objective fate of these small Aβ oligomers burdened with anti-oligomeric Aβ42 antibodies remains to be further studied.

Aβ42 aggregates represent a prominent histopathological feature in AD [26,27]. Many researchers, including ourselves, have long considered Aβ42 as a primary therapeutic target for AD and have believed that immunotherapy against cytotoxic Aβ42 aggregates is a safer and more specific strategy compared with direct inhibition of Aβ42 production, although few success in several clinical trials on anti-Aβ antibody drugs developed for AD to date [28]. We believe that breaking the bottleneck of immunotherapy for AD is just a matter of time. Any attempt to develop antibodies that can effectively reduce the cytotoxicity of Aβ42 aggregates, particularly Aβ42 oligomers and protofibrils, and consequently delay the progression and clinical decline of the disease will be of great significance to advancing the immunotherapy of AD.

5. Conclusion

This study demonstrated that the efficacy of an anti-oligomeric Aβ42 antibody to reduce the cytotoxicity of Aβ42 aggregates appears to be mainly related not only to its affinity for the Aβ42 aggregates, or to its efficacy of slowing or blocking the development of Aβ42 aggregates, but also, and potentially more importantly, to the specific antibody-targeted site or region on the Aβ42 aggregate and to the antibody's binding mode toward the Aβ42 aggregates based on their conformation fit.

Acknowledgments

The authors would like to thank Dr. Tianyu Zhang for help with the computational docking studies. This work was supported by two grants from Jilin Province Science and Technology Department, China (20160204028YY, 20180101262JC).

Appendix A. Supplementary data

Supplementary data to this article can be found online at https://doi.org/10.1016/j.intimp.2018.12.014.

References

[1] E.N. Cline, M.A. Bicca, K.L. Viola, et al., The amyloid-β oligomer hypothesis: beginning of the third decade, J. Alzheimers Dis. 64 (s1) (2018) S567–S610, https://doi.org/10.3233/JAD-179941.
[2] K.L. Viola, W.L. Klein, Amyloid β oligomers in Alzheimer's disease pathogenesis, treatment, and diagnosis, Acta Neuropathol. 129 (2) (2015) 183–206, https://doi.org/10.1007/s00401-015-1386-3.
[3] B.S. Gadad, G.B. Britton, K.S. Rao, Targeting oligomers in neurodegenerative disorders: lessons from α-synuclein, tau, and amyloid-β peptide, J. Alzheimers Dis. 24 (Suppl. 2) (2011) 223–232, https://doi.org/10.3233/JAD-2011-110182.
[4] S. Jeong, Molecular and cellular basis of neurodegeneration in Alzheimer's disease, Mol. Cells 40 (9) (2017) 613–620, https://doi.org/10.4161/pri.22118.
[5] J.M. Nussbaum, M.E. Seward, G.S. Bloom, Alzheimer disease: a tale of two prions, Prion 7 (1) (2013) 14–19, https://doi.org/10.1007/s12010-012-9549-3.
[6] W. Pulawski, U. Ghoshdastider, V. Andrisano, et al., Ubiquitous amyloids, Appl. Biochem. Biotechnol. 166 (7) (2012) 1626–1643, https://doi.org/10.14348/molcells.2017.0096.
[7] Y. Zhang, Y. Sun, Y. Huai, et al., Functional characteristics and molecular mechanism of a new scFv antibody against Aβ42 oligomers and immature protofibrils, Mol. Neurobiol. 52 (3) (2015) 1269–1281, https://doi.org/10.1007/s12035-014-8910-7.
[8] Y. Zhang, X. Chen, J. Liu, et al., The protective effects and underlying mechanism of an anti-oligomeric Aβ42 single-chain variable fragment antibody, Neuropharmacology 99 (2015) 387–395, https://doi.org/10.1016/j.neuropharm.2015.07.038.
[9] X. Huang, J. Wang, L. Cui, et al., Recombinant GST-I-A beta 28-induced efficient serum antibody against A beta 42, J. Neurosci. Methods 186 (1) (2010) 52–59, https://doi.org/10.1016/j.jneumeth.2009.10.026.
[10] L. Cui, X. Huang, J. Wang, et al., Specific and efficient anti-Aβ42 antibodies induced by sixteen tandem repeats of Aβ9, J. Neuroimmunol. 227 (1–2) (2010) 18–25, https://doi.org/10.1016/j.jneuroim.2010.06.004.
[11] B. Friguet, A.F. Chaffotte, L. Djavadiohaniance, et al., Measurements of the true affinity constant in solution of antigen-antibody complexes by enzyme-linked immunosorbent assay, J. Immunol. Methods 77 (2) (1985) 305–319.
[12] B. Friguet, L. Djavadi-Ohaniance, M.E. Goldberg, Some monoclonal antibodies raised with a native protein bind preferentially to the denatured antigen, Mol. Immunol. 21 (7) (1984) 673–677.
[13] L. Jin, X. Yang, Y. Sheng, et al., The second conserved motif in bacterial laccase regulates catalysis and robustness, Appl. Microbiol. Biotechnol. 102 (9) (2018) 4039–4048.
[14] H. Cao, G. Gao, Y. Gu, et al., Trp358 is a key residue for the multiple catalytic activities of multifunctional amylase OPMA-N from *Bacillus* sp. ZW2531-1, Appl. Microbiol. Biotechnol. 98 (5) (2014) 2101–2111, https://doi.org/10.1007/s00253-018-8863-2 (doi: 10.1007/s00253-013-5085-5).
[15] M. Ahmed, J. Davis, D. Aucoin, et al., Structural conversion of neurotoxic amyloid-beta(1-42) oligomers to fibrils, Nat. Struct. Mol. Biol. 17 (5) (2010) 561–567.
[16] R. Aleksis, F. Oleskovs, K. Jaudzems, et al., Structural studies of amyloid-β peptides: unlocking the mechanism of aggregation and the associated toxicity, Biochimie 140 (2017) 176–192, https://doi.org/10.1016/j.biochi.2017.07.011.
[17] B. Murray, B. Sharma, G. Belfort, N-terminal hypothesis for Alzheimer's disease, ACS Chem. Neurosci. 8 (3) (2017) 432–434.
[18] K. Ono, M.M. Condron, D.B. Teplow, Effects of the English (H6R) and Tottori (D7N) familial Alzheimer disease mutations on amyloid beta-protein assembly and toxicity, J. Biol. Chem. 285 (30) (2010) 23186–23197, https://doi.org/10.1002/anie.201402636.
[19] B. Sarkar, V.S. Mithu, B. Chandra, et al., Significant structural differences between transient amyloid-β oligomers and less-toxic fibrils in regions known to harbor familial Alzheimer's mutations, Angew. Chem. 53 (27) (2014) 6888–6892, https://doi.org/10.3233/JAD-2010-1334.
[20] D.G. Smith, G.D. Ciccotosto, D.J. Tew, et al., Histidine 14 modulates membrane binding and neurotoxicity of the Alzheimer's disease amyloid-beta peptide, J. Alzheimers Dis. 19 (4) (2010) 1387–1400, https://doi.org/10.1074/jbc.M109.086496.
[21] C. Söldner, H. Sticht, A. Horn, Role of the N-terminus for the stability of an amyloid-β fibril with three-fold symmetry, PLoS One 12 (10) (2017) e0186347, , https://doi.org/10.1371/journal.pone.0186347.
[22] B.A. Colvin, V.A. Rogers, J.A. Kulas, et al., The conformational epitope for a new Aβ42 protofibril-selective antibody partially overlaps with the peptide N-terminal region, J. Neurochem. 143 (6) (2017) 736–749.
[23] L.A. Kotilinek, B. Bacskai, M. Westerman, et al., Reversible memory loss in a mouse transgenic model of Alzheimer's disease, J. Neurosci. Off. J. Soc. Neurosci. 22 (15)

(2002) 6331–6335, https://doi.org/10.1111/jnc.14211.
[24] B. Mroczko, M. Groblewska, A. Litmanzawadzka, et al., Cellular receptors of amyloid β oligomers (AβOs) in Alzheimer's disease, Int. J. Mol. Sci. 19 (7) (2018) 1884, https://doi.org/10.3390/ijms19071884.
[25] J. Qi, X. Li, H. Peng, et al., Potent and selective antitumor activity of a T cell-engaging bispecific antibody targeting a membrane-proximal epitope of ROR1, Proc. Natl. Acad. Sci. U. S. A. 115 (24) (2018) E5467–E5476, https://doi.org/10.1073/pnas.1719905115.
[26] K. Igor, W.K. Cullen, N.W. Hu, et al., Alzheimer's disease Aβ assemblies mediating rapid disruption of synaptic plasticity and memory, Mol. Brain 5 (1) (2012) 25, https://doi.org/10.1186/1756-6606-5-25.
[27] U. Sengupta, A.N. Nilson, R. Kayed, The role of amyloid-β oligomers in toxicity, propagation, and immunotherapy, EBioMedicine 6 (2016) 42–49, https://doi.org/10.1016/j.ebiom.2016.03.035.
[28] L.S. Honig, B. Vellas, M. Woodward, et al., Trial of solanezumab for mild dementia due to Alzheimer's disease, N. Engl. J. Med. 378 (4) (2018) 321–330.